

Learning to Exploit Elastic Actuators for Quadruped Locomotion

Antonin Raffin¹, Daniel Seidel¹, Jens Kober², Alin Albu-Schäffer¹, João Silvério¹, Frek Stulp¹

Abstract—Spring-based actuators in legged locomotion provide energy-efficiency and improved performance, but increase the difficulty of controller design. While previous work has focused on extensive modeling and simulation to find optimal controllers for such systems, we propose to learn model-free controllers directly on the real robot. In our approach, gaits are first synthesized by central pattern generators (CPGs), whose parameters are optimized to quickly obtain an open-loop controller that achieves efficient locomotion. Then, to make this controller more robust and further improve the performance, we use reinforcement learning to close the loop, to learn corrective actions on top of the CPGs. We evaluate the proposed approach on the DLR elastic quadruped *bert*. Our results in learning trotting and pronking gaits show that exploitation of the spring actuator dynamics emerges naturally from optimizing for dynamic motions, yielding high-performing locomotion, particularly the fastest walking gait recorded on *bert*, despite being model-free. The whole process takes no more than 1.5 hours on the real robot and results in natural-looking gaits.

I. INTRODUCTION

Robots with elastic actuators, such as DLR’s *bert* [1] (Fig. 1), are a promising alternative to their rigid counterparts [2], [3], especially for legged locomotion [4], [5], [6], [7]. In addition to the passive compliance that protects them from collisions, the elastic elements provide energy storing and improved efficiency if properly used. The design of controllers that fully exploit the intrinsic dynamics of compliantly actuated robots remains a challenge, requiring high amounts of time and system-specific knowledge [8]. In this work, we address the problem of obtaining efficient controllers for the locomotion of elastically-actuated robots by formulating controller design as a learning problem.

A. Related Work

Quadruped robots. In recent years, several works studied quadruped locomotion controllers on different hardware platforms (ANYmal, A1 Unitree, ...). Even though some of these have elastic actuators (e.g. ANYmal [9] or Mini Cheetah [10]), their stiffness is high compared to *bert* (see Section II-A) leaving little room to exploit the advantages of the actuators’ elasticity in control.

Reinforcement learning for locomotion. Obtaining locomotion controllers is commonly based on fast simulators and massive parallelism [11], [12] and consists of learning the controllers in simulation and subsequently deploying them on real hardware [13], [14]. Learning in simulation,



Fig. 1: Compliantly actuated DLR quadruped *bert* jumping in place.

however, requires an accurate model of the robot [15], complex reward engineering, and there is no guarantee that a controller working in simulation can be deployed on the real robot. Heavy randomization and generation of diverse training environments help mitigate these issues [16], [12], but still requires engineering efforts to find the right balance between environments too hard to solve and ones that do not transfer to the real robot. Our key difference from many previous approaches is that we learn directly on the real hardware, without the need to transfer from simulation to reality. To our knowledge, this is also the first time that reinforcement learning is used directly on a quadruped with elastic actuators.

Training on real robot. Thanks to more robust hardware [17] and more sample-efficient algorithms [18], [19], [20], [21], learning directly on the real hardware in only a few hours is now possible [22], [23]. Despite these advances, training on real robots can nevertheless be time-consuming and often does not yield natural-looking gaits [19], [20]. In the present work, we aim both at reducing the training time (and thus the robot wear and tear) and obtaining gaits that look natural by 1) providing domain knowledge in the form of central pattern generators and 2) exploiting the natural dynamics of the robot, in particular its elastic joints. In order to mitigate model mismatch or simulation-to-reality gaps, we choose to apply a model-free learning approach directly on the real hardware.

CPGs and Reflex-Based Controllers. Inspired by biology, central pattern generators (CPGs) have been proposed for locomotion [24], [25], [26], [27]. They generate gaits that look natural but require careful parameter tuning, usually done in simulation. In this work, we rely on a CPG model to represent the open-loop motion policy that is later improved with reinforcement learning. Another possibility to obtain

¹ German Aerospace Center (DLR), Robotics and Mechatronics Center (RMC), Münchner Str. 20, 82234 Weßling, Germany

² Delft University of Technology, Cognitive Robotics Department, The Netherlands

dynamic gaits in elastically-actuated robots is to rely on reflex-based controllers [1], [28], [29], whose parameters also require further optimization. Our research is applicable to both CPG and reflex-based controllers, as we automate the parameter optimization and improve robustness and performance with a learned reactive controller. Our approach achieves the fastest walking gait on the *bert* hardware (0.34 m/s vs 0.25 m/s in [28]).

Comparison to CPG-RL and PMTG. Parallel to our work is the CPG-RL method [27], which can be viewed as a special case of Policies Modulating Trajectory Generators (PMTG) [30] where the residual component is removed. In CPG-RL and PMTG, the parameters of the trajectory generator are dynamically updated by an RL agent. Both approaches focus primarily on simulation and therefore rely on domain randomization to ensure performance during real-world testing. Despite sharing architectural similarities, unlike CPG-RL and PMTG, our research emphasizes the unique challenges and benefits associated with learning controllers for quadruped robots with elastic actuators. While CPG-RL employs a massively parallel simulator with 4096 virtual robots, we train directly on a single real robot, concluding that its elastic actuators indeed provide additional robustness and performance over rigid equivalents. Furthermore, we challenge the statement made in the PMTG paper that “*despite the pre-optimization, the TG itself cannot provide stable forward locomotion since it lacks the feedback from the robot*”: our results show that an optimized open-loop controller is sufficient for forward motion on the real hardware.

Feedforward and Feedback Control. The integration of feedforward (open-loop) and feedback (closed-loop) control is a well-established practice in engineering [31], [32], [33], also known as *residual learning* [34] in the RL community. This approach combines the benefits of fast computation and robustness to sensor noise offered by open-loop control with the ability of closed-loop control to address model inaccuracies and respond to disturbances. In our work, we adopt this architecture by utilizing a bio-inspired open-loop control strategy based on central pattern generators (CPGs) and augmenting it with reinforcement learning to enhance performance and robustness. Importantly, *both components of our control system are model-free and optimized directly on the real robot, enabling us to fully leverage the intrinsic dynamics of the elastic robot.*

B. Contributions

In summary, the main contributions of our paper are:

- an approach to design locomotion controllers for robots with elastic actuators (Section III) that combines CPGs, black-box optimization and reinforcement learning, achieving the fastest walking gait for the *bert* platform,
- an experimental verification that the learned controllers exploit the elasticity of the actuators (Section IV), and
- showing that controllers can be learned directly on the real elastic robot in less than one hour, without the need

for complex reward engineering or massively parallel simulation [12] (Section IV).

II. BACKGROUND

In this section, we provide an overview of DLR’s elastic quadruped *bert*, metrics for monitoring spring usage, as well as central pattern generators – a cornerstone of our proposed approach – including the CPG parameters that we aim to optimize.

A. DLR quadruped *bert*

The DLR quadruped *bert* [1] (shown in Fig. 1) is a cat-sized quadruped robot with series elastic actuators (SEA). The legs are attached to the trunk through the hip axis, while the motors are located inside the trunk and connected by belt drives. Each leg consists of a hip and a knee joint and is composed of two segments of equal length of approximately 8cm. The total mass of the robot is about 3.1kg. As depicted in Fig. 2, motors are connected to the links via a linear torsional spring with constant stiffness $k \approx 2.75\text{Nm/rad}$. We use the deflection of the spring to estimate the external torque applied to each joint:

$$\tau_i = k(\theta_i - q_i) \quad (1)$$

where θ is the motor position before the spring and q the joint position.



Fig. 2: Model of the compliantly actuated leg (left) and a serial elastic actuator (right).

bert is equipped with very soft springs relative to its weight and lever arm, i.e. 2.75Nm/rad , compared to for instance StarIETH [9] with 20cm link length, total weight of 23kg and $k=70\text{Nm/rad}$. This means that e.g. when standing in a default position with joints at 30 deg, *bert* can be pushed into joint limits without motor movement, while StarIETH can be pushed into its springs only minimally. This makes *bert* suitable for exploiting its springs as energy storage: forces required to load the springs are quite low and occur during normal gait motions.

When released at the right time, the stored energy can be converted into kinetic energy (joint velocity). This can lead to improved task performance. We formally define metrics to quantify the spring usage in the next section.

B. Metrics

Objective functions of learning methods typically describe tasks (e.g. move forward as fast as possible), and do not enforce explicit usage of the compliant actuators. To measure

if the learned controllers exploit the capability of the elastic robot, we define metrics that quantify the spring usage.

By storing and releasing energy, springs allow joints to reach much higher velocities than the motors [2]. The peak joint velocity usually has a delay compared to the peak motor velocity. Therefore, we propose to compare the ratio between maximum joint and motor velocity over a trajectory for each joint:

$$\mathcal{R}_i^{\dot{\theta}} = \frac{\max_t \dot{q}_i}{\max_t \dot{\theta}_i}. \quad (2)$$

Intuitively, if the springs are fully exploited, the ratio $\mathcal{R}_i^{\dot{\theta}}$ should be greater than one (rigid robot baseline), meaning that the energy is stored and released at the right moment.

Finally, we also monitor the potential and kinetic energy to better understand how energy is transferred and how the learned controllers utilize the elastic actuators. We only consider the kinetic energy related to the task (movement of the center of mass) and therefore do not plot the rotational kinetic energy.

C. Central pattern generators (CPGs) for legged locomotion

CPGs are a common tool used for generating open-loop policies for locomotion [35]. We rely on an implementation based on a system of four coupled nonlinear oscillators [36], [25], [26] (one per leg) that have phase-dependent frequencies. The equation of one oscillator in polar coordinates is [37]:

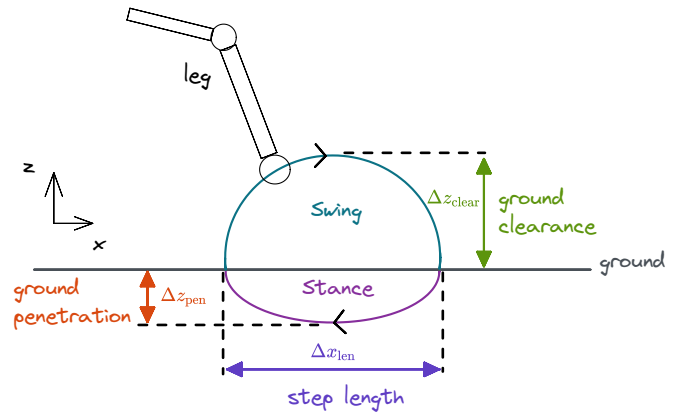
$$\begin{aligned} \dot{\rho}_i &= a(\mu - \rho_i^2)\rho_i \\ \dot{\varphi}_i &= \omega + \sum_j \rho_j c_{ij} \sin(\varphi_j - \varphi_i - \Phi_{ij}) \\ \omega &= \begin{cases} \omega_{\text{swing}} & \text{if } \sin(\varphi_i) > 0 \\ \omega_{\text{stance}} & \text{otherwise} \end{cases} \end{aligned} \quad (3)$$

where ρ_i and φ_i are the amplitude and phase of oscillator i , ω is the frequency of oscillations in rad/s, $\sqrt{\mu}$ is the desired amplitude, ω_{swing} and ω_{stance} are the frequencies of the swing and stance phases. a is a positive constant that controls the rate of convergence to the limit cycle. The weights c_{ij} and phase biases Φ_{ij} define the couplings between oscillators.

The output of each oscillator determines the foot trajectory in Cartesian space (cf. Fig. 3). The coupling matrix Φ therefore determines the gait. For instance, for trotting [38], [39] (foot pattern displayed in Fig. 5), the front right leg is in phase with the hind left leg, and they have a half-cycle offset with the other diagonal (front left with hind right).

As shown in Fig. 3, the trajectory of each leg i depends on four parameters that have to be tuned: ground clearance Δz_{clear} and penetration Δz_{pen} , step length Δx_{len} , swing ω_{swing} and stance ω_{stance} frequencies. We convert the output of one oscillator i to a desired foot trajectory following:

$$\begin{aligned} x_{\text{des},i} &= \Delta x_{\text{len}} \cdot \rho_i \cos(\varphi_i) \\ z_{\text{des},i} &= \Delta z \cdot \rho_i \sin(\varphi_i) \\ \Delta z &= \begin{cases} \Delta z_{\text{clear}} & \text{if } \sin(\varphi_i) > 0 \text{ (swing)} \\ \Delta z_{\text{pen}} & \text{otherwise (stance)}. \end{cases} \end{aligned} \quad (4)$$



Additional parameters: swing and stance duration

Fig. 3: The parameters of the CPG gait that are optimized.

The most critical parameters for an elastically-actuated quadruped are the swing and stance duration, as they should match the natural dynamics of the robot [40], [41].

Tuning these variables manually is time-consuming and usually results in suboptimal choices. Therefore, we automate their tuning using black-box optimization (BBO) and run the optimization directly on the real robot, avoiding any model mismatch. In the following section, we explain the use of BBO and how it fits into our proposed framework.

III. ONLINE LEARNING FOR LEGGED LOCOMOTION

To learn a locomotion controller for the elastic legged robot, we combine two model-free methods. We first optimize the parameters of a selected gait (generated from a CPG) to quickly obtain an open-loop controller that works in the nominal case without disturbances. Then, we refine the controller and make it more robust to perturbations by learning a reinforcement learning (RL) controller that adds offsets to the CPG output. The entire optimization process – depicted in Fig. 4 – is conducted directly on the real robot, removing the need for modeling, accurate simulators or simulation-to-reality transfer.

CPGs provide a compact representation of limb end-effector trajectories (Eq. (4)) that can be adjusted via the set of parameters α shown in Fig. 3:

$$\alpha = \{ \Delta z_{\text{clear}}, \Delta z_{\text{pen}}, \Delta x_{\text{len}}, \omega_{\text{swing}}, \omega_{\text{stance}} \}. \quad (5)$$

A. Open-loop policy learning with black-box optimization (BBO)

In BBO, the goal is to find a set of parameters $\alpha \in \mathbb{R}^n$ that minimizes an objective function $f : \mathbb{R}^n \rightarrow \mathbb{R}$,

$$\alpha^* = \arg \min_{\alpha} f(\alpha). \quad (6)$$

A BBO algorithm only has access to function evaluations of f . It treats f as a black box and does not make any assumption about it (e.g. f can be non-differentiable). In our case, each function evaluation corresponds to one trial (or episode) on the robot for a given set of CPG parameters α .

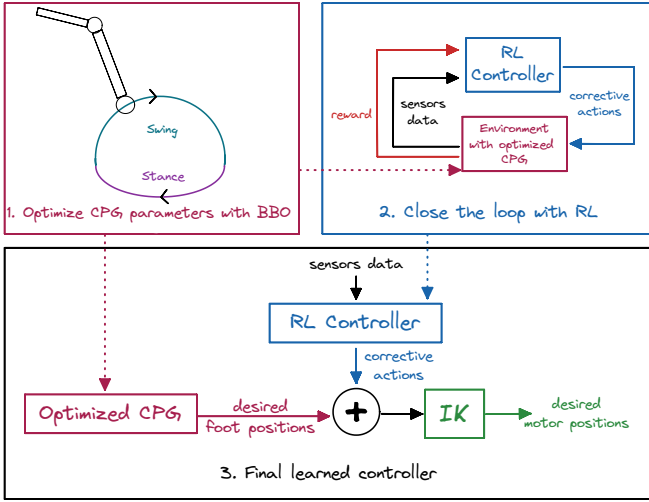


Fig. 4: Overview of the proposed approach: CPG parameters are first optimized using BBO, then a RL controller is trained on top and outputs corrective actions.

We use f to quantify how much a set of CPG parameters satisfies a desired goal. We will describe the objective functions we choose for each task in Section III-C.

B. Closing the loop with reinforcement learning

Reinforcement learning (RL) is similar to BBO but has access to the immediate reward r_t that composes the objective function, when it's available, making it more sample-efficient. Formally, an agent interacts with its environment and generates trajectories ζ_π that follow a policy π . By progressively updating its policy, the agent learns to maximize its cumulative (discounted) reward:

$$\sum_t \mathbb{E}_{\zeta_\pi} [\gamma^t r_t] \quad (7)$$

where $\gamma \in [0, 1)$ is the discount factor and represents a trade-off between maximizing short-term and long-term rewards.

While the BBO algorithm optimizes the parameters of the gait generated by the coupled oscillators, the RL agent learns a reactive controller π as a set of **corrective actions** per leg i defined as $\pi_i = [\pi_{x,i}(s_t), \pi_{z,i}(s_t)]$. The learned policy π adjusts **desired foot positions** produced by the CPG (Eq. (4)) given the current state of the robot s_t , closing the control loop:

$$\begin{aligned} x_{\text{des},i} &= \Delta x_{\text{len}} \cdot \rho_i \cos(\varphi_i) + \pi_{x,i}(s_t) \\ z_{\text{des},i} &= \Delta z \cdot \rho_i \sin(\varphi_i) + \pi_{z,i}(s_t) \end{aligned} \quad (8)$$

C. Task Specification

In this work, we focus on two dynamic gaits: trotting and pronking (jumping in place).

a) Trotting: The first task we are interested in is to obtain a fast walking trot, where we optimize for mean forward speed ($f(\alpha) = -\frac{\Delta x}{\Delta t}$). We define the immediate reward as the distance traveled between two timesteps along the desired axis ($r_t = \dot{x}_{\text{robot}}$).

After optimization, we further evaluate the five best performing candidates for more episodes. This post-processing step is key to filtering out the evaluation noise, i.e. it helps to find parameters that lead to reliable gaits.

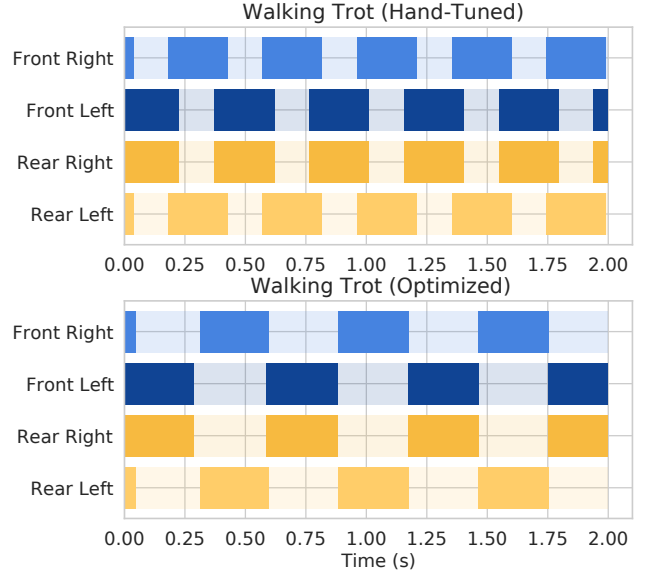


Fig. 5: Trotting gaits for a 2-second period. Dark colors represent stance phases, light colors swing phases.

b) Pronking: The second task is to jump in place (pronk) without falling or drifting from the starting position. In a pronking gait, all legs are synchronized: they all take off and land at the same time (as seen in Fig. 6). The step length is set to zero in that case. We penalize angular velocity for roll and yaw, distance to the starting point and reward velocity along the z axis (aligned with gravity field): $r_t = w_1 |\dot{z}| - w_2 (\dot{\psi}_{\text{roll}}^2 + \dot{\psi}_{\text{yaw}}^2) - w_3 \Delta_{xy}^2$, where $w_{1,2,3}$ are weights chosen in a way that the primary reward $|\dot{z}|$ has a higher magnitude than the secondary costs. We define the objective function for the BBO as the total reward per episode ($f(\alpha) = -\sum_t r_t$).

In all tasks, the RL agent receives as input s_t the current joint positions, velocities, torques, linear acceleration and angular velocity (from the IMU), and the desired foot position generated by the CPG controller. The action space corresponds to offsets for each foot in Cartesian space.

IV. RESULTS

We evaluate our approach on two locomotion tasks (trotting and pronking) to answer the following questions:

- Can we quickly learn a controller directly on the real elastic robot?
- How does the learned controller exploit the elastic actuators?
- What do we gain by learning CPG parameters with BBO?
- What is the added value of closing the loop with RL?
- Is CPG needed or is RL from scratch enough?

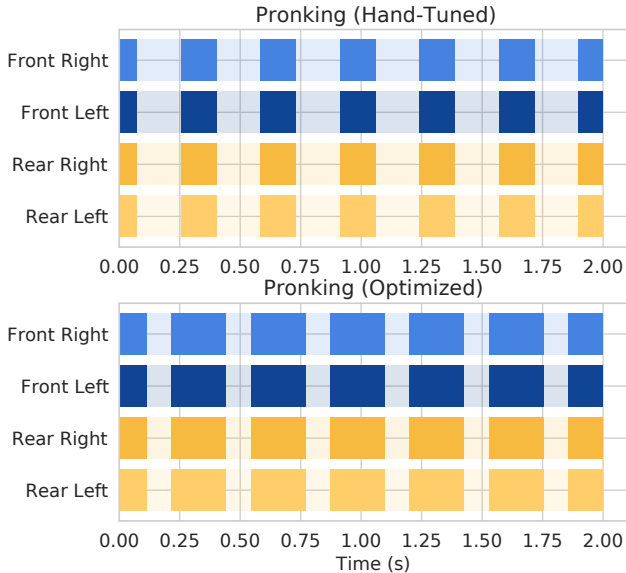


Fig. 6: Pronking gaits for a 2-second period.

A. Setup

During training only, we use an external tracking system that provides robot absolute position and orientation at 60Hz. Each trial has a timeout of 5s and terminates earlier if the robot reaches the tracking limits or if the quadruped falls over. We use a treadmill of one by three meters to limit the need of manual intervention. The treadmill is also the tracked area usable by the robot.

To tune the parameters of the open-loop controller, we use Bayesian optimization, as it is sample efficient in low-dimensional search spaces [22]. We use the TPE [42] implementation from the Optuna [43] library. For reinforcement learning we choose TQC, a sample-efficient off-policy algorithm [44], with smooth exploration [23] to remove the need for a low-pass filter. We run RL experiments using the RL Zoo [45] framework and Stable-Baselines3 [46] library (with tuned hyperparameters from [23]).

The agent is trained at 30Hz but can be evaluated at 60Hz (limited by the tracking system). The CPG parameters are optimized during 45 minutes for the trotting experiment and 25 minutes for the pronking one (250 and 160 trials respectively). The RL controller is then trained on top during one hour. For safety, the motor velocities are capped at $\dot{\theta}_{\max} = 4\text{rad/s}$.

Hand-tuned Baseline. We use parameters tuned by hand by a human experimenter familiar with the elastic quadruped as a baseline. The experimenter was given the same time and search space as the BBO algorithm, as well as an explanation of the meaning and importance of each parameter.

RL Baseline. When learning from scratch, we use the setting described in [19] to be able to learn a controller in minutes, using 10 gradient steps per control step. The action space is extended to be similar in task space to the one used by the CPG controller.

B. Fast Trotting

Without the need for a simulator or prior knowledge, the automatic tuning with BBO quickly finds good parameters for trotting in less than an hour with the real robot. Looking at the optimization history in Fig. 7, the algorithm discovers parameters that match the hand-tuned performance in less than 5 minutes (30 trials, a trial takes around 10s on average, accounting for resets) and parameters that exceed 0.20m/s in 10 minutes (60 trials).

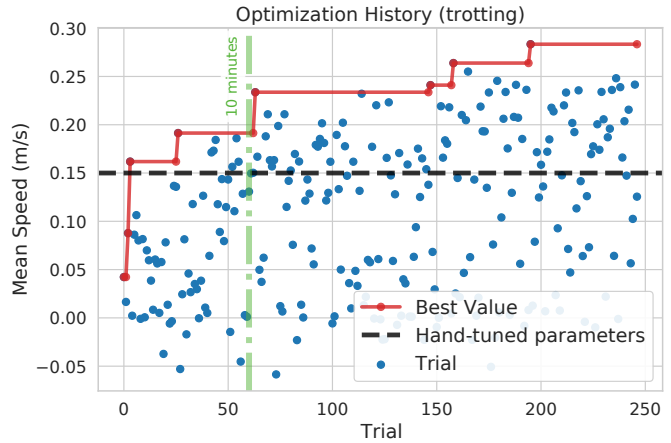


Fig. 7: Optimization history plot for trotting (45 minutes).

After only 40 minutes of optimization, the gains are significant for the trotting gait (cf. Table I): with the same maximum motor velocity, the quadruped trots 70% faster, reaching a mean speed of 0.26m/s (vs. 0.15m/s with hand-tuned parameters).

Closing the loop with reinforcement learning helps to further improve performance¹. Both with the hand-tuned and the optimized CPG, the robot trots significantly faster (20% and 30% faster respectively). The combination of optimized CPG + RL gives the best results (0.34m/s), and the hand-tuned CPG + RL does not reach the performance of the optimized CPG gait (0.19m/s). This is also the fastest walking speed achieved on the *bert* platform (the previous record was 0.25 m/s in [28]).

	RL	CPG		CPG + RL	
		hand-tuned	optimized	hand-tuned	optimized
Speed (m/s) \uparrow	0.14	0.15	0.26	0.19	0.34
Mean $\mathcal{R}_{\dot{\theta}}$ \uparrow	1.4 +/- 0.1	1.4 +/- 0.1	1.9 +/- 0.1	1.6 +/- 0.1	2.0 +/- 0.3

TABLE I: Results for the fast trotting experiment. The optimized gait trots 70% faster than the hand-tuned controller and exploits more the springs. RL from scratch merely achieves the hand-tuned CPG performance. RL on top of CPG further improves the performance.

We display in Fig. 5 the patterns and in Figs. 8a and 8b the trotting gaits for the hand-tuned and optimized parameters (CPG only). The main difference is a longer swing phase (0.29s vs. 0.14s for the hand-tuned one) and larger step length ($\Delta x_{\text{len}}=5\text{cm}$ vs. 2.5cm). However, increasing the

¹We used bootstrap confidence intervals to test for statistical significance.

step length alone does not result in a faster gait. Only in combination with appropriate adjustment of the other parameters, the speed can be increased.

Concerning joint and motor velocities, the optimized controller reaches higher peak joint velocities for the same peak motor velocities (Table I). The peak joints velocities are almost twice the one of the motors ($\mathcal{R}_{\dot{\theta}}^{\dot{q}}=2.0$ vs. 1.4 for the hand-tuned) showing the potential of springs for locomotion. In fact, as seen in Fig. 9, the peak in joint velocity \dot{q} corresponds to a sudden decrease in the spring potential energy: the energy of the spring is converted into kinetic energy. The main difference between the results of hand-tuned and optimized parameters is the timing of this conversion. For the learned controller, it happens when the motor velocity $\dot{\theta}$ is still at its peak [B], while for the hand-tuned one, it happens when the motor velocity has already started to decrease [A].



(a) Hand-tuned trotting gait (0.15m/s).



(b) Optimized trotting gait (0.26m/s).

Fig. 8: Hand-tuned and optimized trotting gaits for a 2-second period.

C. Is RL from scratch sufficient?

Table I also shows the result of learning to walk from scratch with RL on the real robot. As shown in the accompanying video, the RL controller learns to walk in 10 minutes only, but the performance plateaus afterward. The RL controller barely reaches the hand-tuned CPG performance (0.14m/s), and this translates into less use of the springs ($\mathcal{R}_{\dot{\theta}}^{\dot{q}} \approx 1.4$).

This experiment illustrates the shortcomings of learning from scratch. RL would require extensive reward engineering [13], [11] to achieve natural-looking gaits similar to the open-loop CPG (e. g. adding a foot clearance reward). The gait learned by RL is also unpredictable: since we only optimize for the forward speed, it does not have to trot, but could for example, prnk. On the other hand, the gaits produced by the CPG controller encode basic primitives for walking (e. g. foot clearance does not need to be specified in the reward), and the coupling matrix gives control over the gait type. Learning from scratch with RL is more dangerous for the hardware, as any kind of movement of the legs

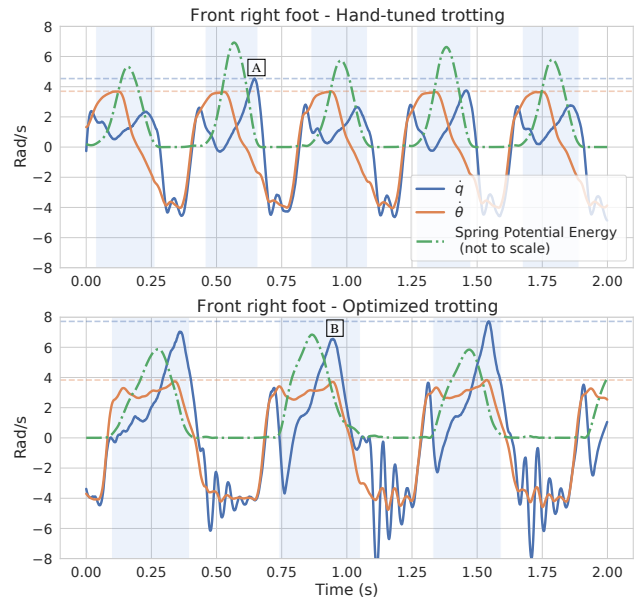


Fig. 9: Joint and motor velocity of the front right foot while trotting for a 2-second period. Darker background represents stance phase. Blue and orange dotted lines represent maximum joint and motor velocities, respectively.

is allowed, and the smoothness of the controller must be enforced to not damage the motors with high frequency control output.

Finally, we do not consider approaches that train a controller in simulation [12], [11]. We want to fully exploit the real robot dynamics and be able to quickly reuse the approach on other robots without the expensive cost of bridging the gap between simulation and reality each time.

D. Stabilizing Pronking

For the pronking task, the BBO algorithm discovers multiple good sets of parameters in less than 10 minutes (60 trials), as seen in the optimization history in Fig. 10. The hand-tuned and optimized CPG parameters both allow the robot to jump in place, but the open-loop controller rapidly fails when the robot roll angle increases, either as a consequence of an applied perturbation or the interaction with the floor.

By closing the loop between the robot state and actions, the reinforcement learning controller helps mitigate this issue, as summarized in Table II. Here we see that the solution with RL results in no failures. The qualitative difference is highlighted in the accompanying video. The quadruped also jumps more in place (less drift with respect to the starting position) while keeping the same jumping height.

As for the trotting experiment, adding RL on top of the hand-tuned CPG improves performance but does not match the optimized controller.

We show in Fig. 6 the patterns for the hand-tuned and optimized pronking gaits (CPG only), and in Fig. 11 the robot jumping in place. The optimized parameters are quite different from the hand-tuned ones: the swing phase is shorter (0.10s vs. 0.18s for the hand-tuned one) and stance

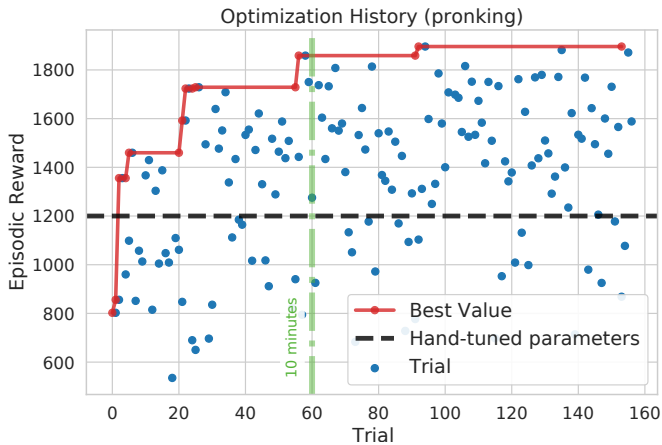


Fig. 10: Optimization history plot for pronking (30 minutes).

phase longer (0.22s vs. 0.15s), and the ratio between the two is inverted (swing phase shorter than the stance phase).

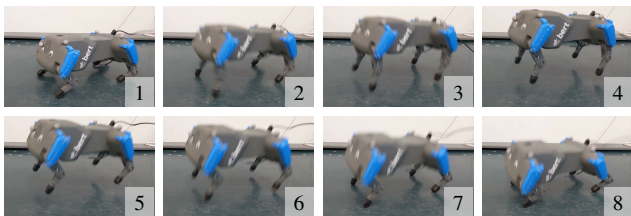


Fig. 11: Pronking gait (max jump height: 0.1m).

The energy evolution in Fig. 12 demonstrates how elastic properties of the actuators are exploited. The robot first crouches on the floor (decrease in gravitational potential energy), compressing and loading the spring [C]. To jump, it then pushes all its legs against the floor, while at the same time releasing the energy stored in the springs. This energy is converted both into kinetic energy (the robot reaches its maximum speed shortly after takeoff [D]) and gravitational potential energy. After reaching the maximum height [E], the gravitational potential energy is converted back into kinetic energy before the robot lands and the jumping cycle starts again.

The main difference between the hand-tuned and optimized parameters is the maximum spring potential energy. This results in higher jumps for the optimized controller (higher peak in gravitational potential energy in Fig. 12). Finally, compared to trotting, the peak joint velocity is higher for pronking ($\mathcal{R}_{\dot{\theta}}^{\frac{1}{2}}=3.5$ vs. 1.8) as the leg springs are synchronously compressed and released. As shown in Table II, the peak joint velocity is on average 3.5 the maximum velocity reached by the motors for the optimized parameters, versus 2.9 for the hand-tuned ones.

V. CONCLUSION

We have shown that by integrating central pattern generators with black-box optimization and reinforcement learning, it is possible to learn efficient and natural-looking gaits directly on a real elastic quadruped robot. This is done without the need for complex reward engineering or massively

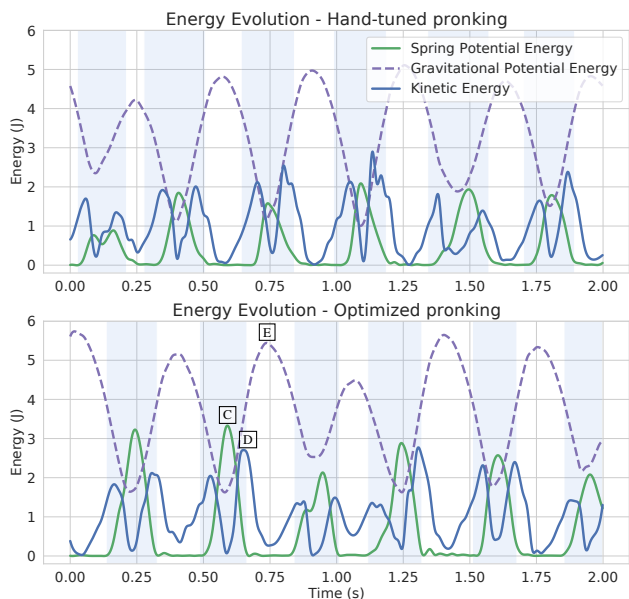


Fig. 12: Energy evolution while pronking for a 2-second period.

	CPG		CPG + RL	
	hand-tuned	optimized	hand-tuned	optimized
Mean reward (10^3) \uparrow	1.0 +/- 0.1	1.4 +/- 0.2	1.4 +/- 0.1	1.6 +/- 0.1 (+60%)
Drift Δ_{xy} cost \downarrow	1.3 +/- 0.1	1.5 +/- 0.1	1.3 +/- 0.1	1.3 +/- 0.1
Angular vel. cost \downarrow	204 +/- 6	194 +/- 14	183 +/- 10	160 +/- 10
Max height (cm) \uparrow	7.3	9.3	8.1	9.4
Failures	1 failure	1 failure	no failure	no failure
Mean $\mathcal{R}_{\dot{\theta}}^{\frac{1}{2}}$ \uparrow	2.9 +/- 0.2	3.3 +/- 0.2	3.2 +/- 0.2	3.5 +/- 0.3 (+20%)

TABLE II: Results for the jumping in place experiment, on 5 evaluation episodes. Failures occur without external perturbations.

parallel simulation. In particular, the learned gaits exploit the natural dynamics of the robot, enabling efficient storage and release of energy in the springs, a behavior that emerged naturally during training without needing to be accounted for in the reward. This enabled DLR’s quadruped *bert* to achieve the fastest walking speed ever recorded.

Learning directly on the real robot comes with its own challenges. Each experiment must be carefully designed to achieve sample efficient training (choice of action and search space, hyperparameters); trials on the real robot cannot be parallelized. Like simulation-to-reality approaches, running software on real hardware requires expertise to ensure the robot’s safety and is time-consuming. However, with our approach, once training is complete, no additional step is required for deployment. Although we focus here on individual gaits, our future research will address the discovery of novel behaviors, especially when adapting to new and unseen environments.

ACKNOWLEDGMENT

This work was funded by the EU’s H2020 Research and Innovation Programme under grant numbers 951992 (VeriDream) and 835284 (M-Runners). We thank Milan Hermann and Florian Loeffl for their help with the hardware.

REFERENCES

- [1] D. Seidel, M. Hermann, T. Gumpert, F. C. Loeffl, and A. Albu-Schäffer, "Using elastically actuated legged robots in rough terrain: Experiments with DLR quadruped bert," in *2020 IEEE Aerospace Conference*, 2020, pp. 1–8.
- [2] N. Mansfeld, M. Keppler, and S. Haddadin, "Speed gain in elastic joint robots: An energy conversion-based approach," *IEEE Robotics and Automation Letters*, vol. 6, no. 3, pp. 4600–4607, 2021.
- [3] F. Bjelonic, J. Lee, P. Arm, D. Sako, D. Tateo, J. Peters, and M. Hutter, "Learning-based design and control for quadrupedal robots with parallel-elastic actuators," *IEEE Robotics and Automation Letters*, 2023.
- [4] R. M. Alexander, "Three uses for springs in legged locomotion," *The International Journal of Robotics Research*, vol. 9, no. 2, pp. 53–61, 1990.
- [5] M. Grimmer, M. Eslamy, S. Gliech, and A. Seyfarth, "A comparison of parallel- and series elastic elements in an actuator for mimicking human ankle joint in walking and running," in *2012 IEEE International Conference on Robotics and Automation*, 2012, pp. 2463–2470.
- [6] F. Ruppert and A. Badri-Spröwitz, "Learning plastic matching of robot dynamics in closed-loop central pattern generators," *Nature Machine Intelligence*, vol. 4, no. 7, pp. 652–660, 2022.
- [7] P. Kormushev, B. Ugurlu, D. G. Caldwell, and N. G. Tsagarakis, "Learning to exploit passive compliance for energy-efficient gait generation on a compliant humanoid," *Autonomous Robots*, vol. 43, no. 1, pp. 79–95, 2019.
- [8] M. Keppler, D. Lakatos, C. Ott, and A. Albu-Schäffer, "Elastic structure preserving (esp) control for compliantly actuated robots," *IEEE Transactions on Robotics*, vol. 34, no. 2, pp. 317–335, 2018.
- [9] M. Hutter, C. Gehring, M. Bloesch, M. A. Hoepflinger, C. D. Remy, and R. Siegwart, "StarLETH: A compliant quadrupedal robot for fast, efficient, and versatile locomotion," in *Adaptive Mobile Robotics*. World Scientific, 2012, pp. 483–490.
- [10] B. Katz, J. D. Carlo, and S. Kim, "Mini cheetah: A platform for pushing the limits of dynamic quadruped control," *2019 International Conference on Robotics and Automation (ICRA)*, pp. 6295–6301, 2019.
- [11] T. Miki, J. Lee, J. Hwangbo, L. Wellhausen, V. Koltun, and M. Hutter, "Learning robust perceptive locomotion for quadrupedal robots in the wild," *Science Robotics*, vol. 7, no. 62, p. eabk2822, 2022.
- [12] N. Rudin, D. Hoeller, P. Reist, and M. Hutter, "Learning to walk in minutes using massively parallel deep reinforcement learning," in *Conference on Robot Learning*. PMLR, 2022, pp. 91–100.
- [13] J. Lee, J. Hwangbo, L. Wellhausen, V. Koltun, and M. Hutter, "Learning quadrupedal locomotion over challenging terrain," *Science robotics*, vol. 5, no. 47, p. eabc5986, 2020.
- [14] A. Kumar, Z. Fu, D. Pathak, and J. Malik, "Rma: Rapid motor adaptation for legged robots," 2021.
- [15] J. Hwangbo, J. Lee, A. Dosovitskiy, D. Bellicoso, V. Tsounis, V. Koltun, and M. Hutter, "Learning agile and dynamic motor skills for legged robots," *Science Robotics*, vol. 4, no. 26, p. eaau5872, 2019.
- [16] Z. Fu, A. Kumar, J. Malik, and D. Pathak, "Minimizing energy consumption leads to the emergence of gaits in legged robots," 2021.
- [17] D. Büchler, S. Guist, R. Calandra, V. Berenz, B. Schölkopf, and J. Peters, "Learning to play table tennis from scratch using muscular robots," *IEEE Transactions on Robotics*, 2022.
- [18] K. Chatzilygeroudis, V. Vassiliades, F. Stulp, S. Calinon, and J.-B. Mouret, "A survey on policy search algorithms for learning robot controllers in a handful of trials," *IEEE Transactions on Robotics*, vol. 36, no. 2, pp. 328–347, 2019.
- [19] L. Smith, I. Kostrikov, and S. Levine, "A walk in the park: Learning to walk in 20 minutes with model-free reinforcement learning," 2022.
- [20] P. Wu, A. Escontrela, D. Hafner, K. Goldberg, and P. Abbeel, "Daydreamer: World models for physical robot learning," 2022.
- [21] T. Hiraoka, T. Imagawa, T. Hashimoto, T. Onishi, and Y. Tsuruoka, "Dropout q-functions for doubly efficient reinforcement learning," in *International Conference on Learning Representations*, 2022.
- [22] R. Calandra, A. Seyfarth, J. Peters, and M. P. Deisenroth, "Bayesian optimization for learning gaits under uncertainty," *Annals of Mathematics and Artificial Intelligence*, vol. 76, no. 1, pp. 5–23, 2016.
- [23] A. Raffin, J. Kober, and F. Stulp, "Smooth exploration for robotic reinforcement learning," in *Conference on Robot Learning*, 2021.
- [24] A. Crespi and A. J. Ijspeert, "Online optimization of swimming and crawling in an amphibious snake robot," *IEEE Transactions on Robotics*, vol. 24, no. 1, pp. 75–87, 2008.
- [25] L. Righetti and A. Ijspeert, "Pattern generators with sensory feedback for the control of quadruped locomotion," in *2008 IEEE International Conference on Robotics and Automation*. Pasadena, USA: IEEE, 2008, pp. 819–824.
- [26] M. Ajallooeian, S. Pouya, A. Sproewitz, and A. J. Ijspeert, "Central pattern generators augmented with virtual model control for quadruped rough terrain locomotion," in *2013 IEEE international conference on robotics and automation*. IEEE, 2013, pp. 3321–3328.
- [27] G. Bellegarda and A. J. Ijspeert, "CPG-RL: Learning central pattern generators for quadruped locomotion," *IEEE Robotics and Automation Letters*, 2022 (Accepted).
- [28] D. Lakatos, K. Ploeger, F. Loeffl, D. Seidel, F. Schmidt, T. Gumpert, F. John, T. Bertram, and A. Albu-Schäffer, "Dynamic locomotion gaits of a compliantly actuated quadruped with slip-like articulated legs embodied in the mechanical design," *IEEE Robotics and Automation Letters*, vol. 3, no. 4, pp. 3908–3915, 2018.
- [29] A. Schmidt, B. Feldotto, T. Gumpert, D. Seidel, A. Albu-Schäffer, and P. Stratmann, "Adapting highly-dynamic compliant movements to changing environments: A benchmark comparison of reflex-vs. cpg-based control strategies," *Frontiers in Neurobotics*, vol. 15, 2021.
- [30] A. Iscen, K. Caluwaerts, J. Tan, T. Zhang, E. Coumans, V. Sindhwani, and V. Vanhoucke, "Policies modulating trajectory generators," in *Conference on Robot Learning*. PMLR, 2018, pp. 916–926.
- [31] G. C. Goodwin, S. F. Graebe, and M. E. Salgado, *Control System Design*, 1st ed. USA: Prentice Hall PTR, 2000.
- [32] K. J. Astrom and R. M. Murray, *Feedback Systems: An Introduction for Scientists and Engineers*. USA: Princeton University Press, 2008.
- [33] C. Della Santina, M. Bianchi, G. Grioli, F. Angelini, M. Catalano, M. Garabini, and A. Bicchi, "Controlling soft robots: balancing feedback and feedforward elements," *IEEE Robotics & Automation Magazine*, vol. 24, no. 3, pp. 75–83, 2017.
- [34] T. Johannink, S. Bahl, A. Nair, J. Luo, A. Kumar, M. Loskyll, J. A. Ojea, E. Solowjow, and S. Levine, "Residual reinforcement learning for robot control," in *2019 International Conference on Robotics and Automation (ICRA)*. IEEE, 2019, pp. 6023–6029.
- [35] A. J. Ijspeert, "Central pattern generators for locomotion control in animals and robots: A review," *Neural Networks*, vol. 21, no. 4, pp. 642–653, 2008, robotics and Neuroscience.
- [36] L. Righetti, J. Buchli, and A. J. Ijspeert, "Dynamic hebbian learning in adaptive frequency oscillators," *Physica D: Nonlinear Phenomena*, vol. 216, no. 2, pp. 269–281, 2006.
- [37] A. J. Ijspeert, A. Crespi, D. Ryczko, and J.-M. Cabelguen, "From swimming to walking with a salamander robot driven by a spinal cord model," *science*, vol. 315, no. 5817, pp. 1416–1420, 2007.
- [38] M. Hildebrand, "Symmetrical gaits of horses," *Science*, vol. 150, no. 3697, p. 701–708, 1965.
- [39] Z. E. Bhatti, "Gait analysis and biomechanics of quadruped motion for procedural animation and robotic simulation," 2017.
- [40] C. Della Santina, D. Lakatos, A. Bicchi, and A. Albu-Schaeffer, "Using nonlinear normal modes for execution of efficient cyclic motions in articulated soft robots," in *International Symposium on Experimental Robotics*. Springer, 2020, pp. 566–575.
- [41] A. Albu-Schäffer and C. Della Santina, "A review on nonlinear modes in conservative mechanical systems," *Annual Reviews in Control*, vol. 50, pp. 49–71, 2020.
- [42] J. Bergstra, R. Bardenet, Y. Bengio, and B. Kégl, "Algorithms for hyper-parameter optimization," in *Advances in Neural Information Processing Systems*, J. Shawe-Taylor, R. Zemel, P. Bartlett, F. Pereira, and K. Weinberger, Eds., vol. 24. Curran Associates, Inc., 2011.
- [43] T. Akiba, S. Sano, T. Yanase, T. Ohta, and M. Koyama, "Optuna: A next-generation hyperparameter optimization framework," in *Proceedings of the 25th ACM SIGKDD International Conference on Knowledge Discovery & Data Mining*, ser. KDD '19. New York, NY, USA: Association for Computing Machinery, 2019, p. 2623–2631.
- [44] A. Kuznetsov, P. Shvechikov, A. Grishin, and D. Vetrov, "Controlling overestimation bias with truncated mixture of continuous distributional quantile critics," in *Proceedings of the 37th International Conference on Machine Learning*, ser. ICML'20. JMLR.org, 2020.
- [45] A. Raffin, "RI baselines3 zoo," 2020.
- [46] A. Raffin, A. Hill, A. Gleave, A. Kanervisto, M. Ernestus, and N. Dormann, "Stable-baselines3: Reliable reinforcement learning implementations," *Journal of Machine Learning Research*, vol. 22, no. 268, pp. 1–8, 2021.